Performance analysis of full-duplex 4×10Gbps TWDM-PON using QAM-OFDM modulation

MEET KUMARI[a,*], REECHA SHARMA[a], ANU SHEETAL[b]
aDepartment of Electronics and Communication Engineering, Punjabi University, Patiala, India
bDepartment of Electronics and Communication Engineering, Guru Nanak Dev University Regional Campus, Gurdaspur, India

In this paper, a bidirectional 40/40Gbps time and wavelength division multiplexing-passive optical network (TWDM-PON) system employing 4-level quadrature amplitude modulation (4-QAM) orthogonal frequency division multiplexing (OFDM) modulation is proposed and analysed to ulfil the high bandwidth demand of next-generation access networks. The system has been analysed for variable distance, data rate and input power. The results show that the bidirectional 40/40 Gbps traffic can be transmitted successfully up to 200 km with an optimum input power of 16 dBm at $3.8{\times}10^{-3}$ bit error rate (BER) using digital signal processing (DSP) unit. Also, the proposed system shows its superiority as compared to previous work.

1. Introduction

High-speed and high-bandwidth passive optical networks (PONs) are emerging access networks to provide broadband access to consumers economically. However, for the future next-generation passive optical networks (NG-PONs), the bidirectional data rate of 40 Gbps, or even beyond 100 Gbps is required due to different broadband multi-service requirements [1]. Thus to achieve a high access rate in PON to satisfy the increasing demand of large capacity, an NG-PON stage 2 (NG-PON2) based bidirectional 40 Gbps time and wavelength division multiplexing PON (TWDM-PON) access network has been chosen by full-service access network (FSAN) in 2012. several TWDM-PONs have been designed and demonstrated to support the 40 Gbps information rate [2]. As the emergence of end-users' demand, the primary goal of next-future high-bandwidth NG-PON system is to allow a large number of users to access traffic at a high data rate over long-reach distance [3].

Further, to acquire 100Gbps with TWDM design, various solutions for the upstream and downstream modulation format, like 4-level pulse amplitude modulation (4-PAM), on-off keying (OOK) and duobinary have been proposed and investigated [4]. Lin, B. et al. in [5] proposed and demonstrated an asymmetric TWDM-PON with 100 Gbps downstream double side-band orthogonal frequency-division multiplexing (DSB OFDM) modulation and 40 Gbps upstream OOK modulation utilizing reflective semiconductor optical amplifier (RSOA) at user end for 20 km fiber distance. Šprem, M. and Babić, D. in [6] proposed and demonstrated the

symmetric wavelength division multiplexing PON (WDM-PON) with 55 Gbps downstream and upstream OOK modulation with channel spacing of 100 GHz and 50 GHz at 30 km distance. Tang, X in [7] proposed and investigated 40 Gbps 4-PAM PON with low-complexity equalizers at 20 km distance. Zhang, W. F in [8] proposed and demonstrated symmetric 10 Gbps WDM-PON with differential quadrature phase-shift keying (DQPSK) modulation and upstream OOK modulation at 20 km distance. Shao, Y in [9] proposed and simulated symmetric 10 Gbps PON with 4-PAM and demodulation at 20 km distance. Thus, for the 40 Gbps-100 Gbps PON access using 4-PAM, OOK and duobinary on single wavelength in standard 20 km PON reach are not much more realizable because of the optical fiber constraints such as polarization mode dispersion, chromatic dispersion (CD) and pricey 40 GHz transceivers [4,10].

For the future 40 Gbps to 100 Gbps PON, to achieve a higher data rate economically, the high spectrum efficiency quadrature amplitude modulation OFDM (QAM-OFDM) modulation would be used [11]. Recently, a 100 Gbps downstream and 40 Gbps upstream asymmetric TWDM-PON have been analyzed by utilizing broadband QAM-OFDM signal. Although they required a re-modulation scheme at ONU for upstream channels using an electro-absorption modulator (EAM) and higher-order of sampling rate for OFDM processing [12]. Also, the OFDM subcarriers would be influenced by the higher frequency owing to the radio frequency (RF) power fading and CD.

QAM-OFDM is a spectrally efficient modulation format that encodes the data on multiple orthogonal

subcarriers. Contrarily, time-division multiplexing (TDM) and WDM support time and wavelength multiplexing of distinct channels respectively; hence permitting several consumers to access and share the single transmission link. Apart from TDM and WDM, OFDM can allow dynamic bandwidth allocation, a better degree of freedom, and software reconfigurable [13,14]. Thus, NG-PON2 based hybrid TWDM-PON using 4-QAM modulation format offers high capacity, high-speed transmission and high security.

In this paper, the symmetrical and full-duplex TWDM-PON with 40 Gbps (4×10 Gbps) downstream and 40Gbps upstream OFDM modulation using four pairs of wavelengths is proposed. The proposed TWDM-PON with OFDM modulation is operated within 15 GHz bandwidth and each OFDM band is modulated at the 4-QAM format. Here, coherent detection is employed to provide excellent frequency selectivity as well as receiver sensitivity. The main novelties of proposed bidirectional 40/40 Gbps TWDM-PON using 4-QAM-OFDM modulation architecture are as followings: [4], [15]

1. Allowing distinct subscribers to access and share the same communication channel by using QAM-OFDM modulation format in TWDM-PON architecture.

2. To allow more degree of freedom via OFDM as compared to TDM and WDM multiplexing.
3. TWDM/OFDM-PON offers several novel advantages such as dynamic bandwidth allocation, maximum spectral efficiency and software-reconfigurable.
4. To compensate CD induced transmission impairments by utilizing frequency domain equalization (FDE) method for OFDM in the proposed system.

Here, in Section 2, the proposed system design is introduced. Section 3 illustrates the results and discussion, followed by the conclusion in Section 4.

2. Proposed bidirectional TWDM-PON using OFDM modulation architecture

Fig. 1 illustrates the proposed TWDM-PON architecture. Here, in the optical line terminal (OLT), four pairs of CW frequencies ({187.8, 195.6}, {187.7, 195.5}, {187.6, 195.4} and {187.5, 195.3}) in THz having 100 GHz of channel spacing used for 40 Gbps downstream and 40G bps upstream signals in the system.
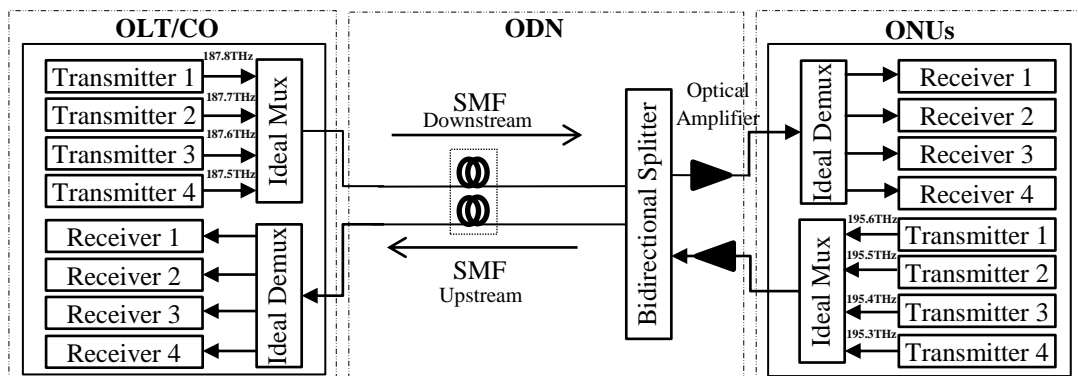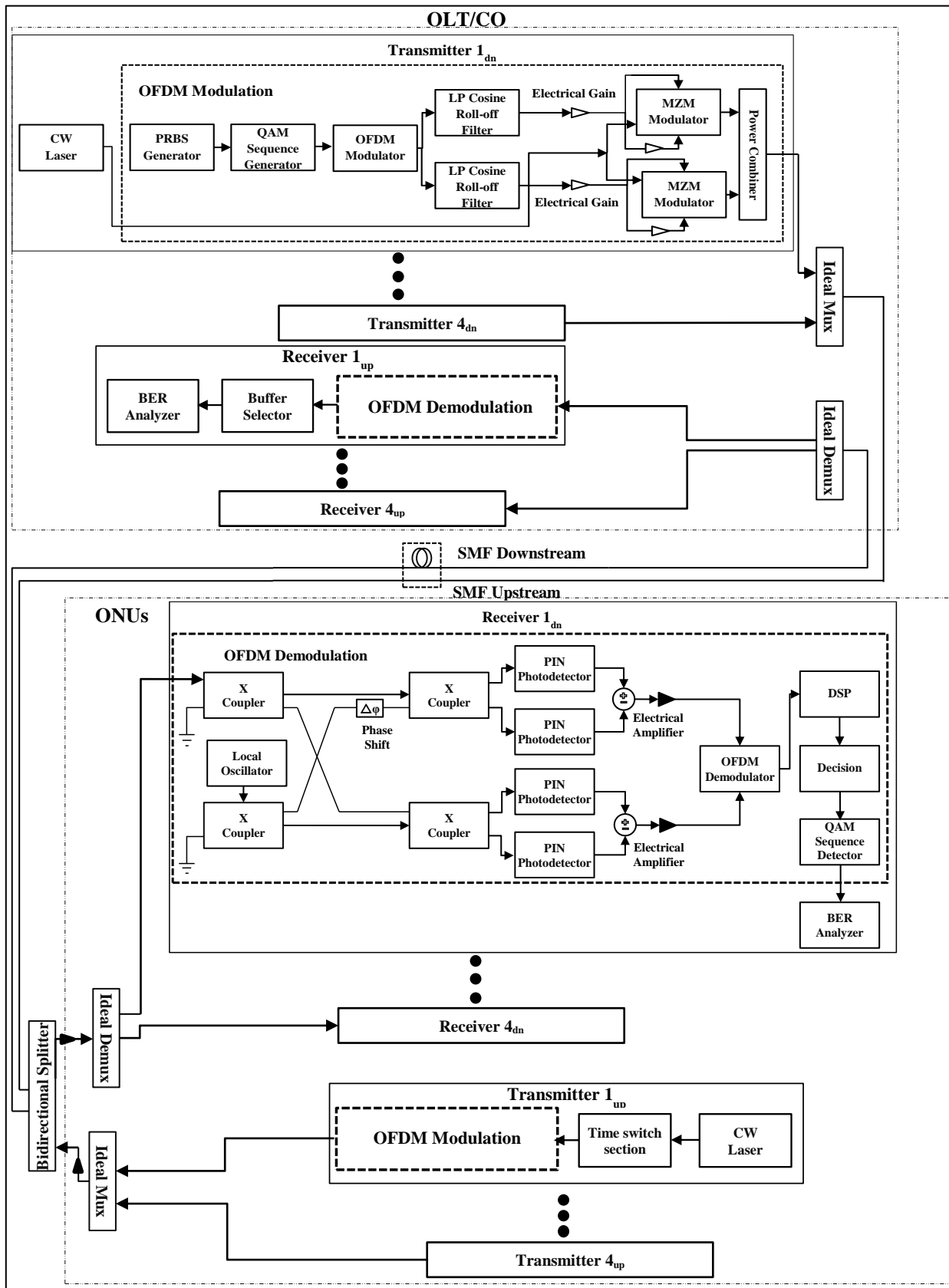

Fig. 1. Schematic of bidirectional 4×10 Gbps hybrid TWDM-OFDM PON transmitter-receiver

As shown in Fig. 1, in the downstream transmission, the four downstream frequencies with modulated OFDM signals are multiplexed by the ideal multiplexer and then passed through downstream single-mode fiber (SMF) followed by a bidirectional splitter. After amplification by an optical amplifier, the downstream signals are distributed to optical network units (ONUs) by an ideal de-multiplexer [15]. At the ONUs, the receiver prefers its definite wavelength and then decodes the OFDM signal. In the upstream transmission, each ONU transmits boosted OFDM signals by an optical amplifier with assigned frequencies transmitted through upstream SMF. At the central office (CO), the upstream signals are de-multiplexed and decoded by an allocated upstream

receiver. Compared with 16-QAM and 64-QAM, 4-QAM can lessen the requirement of signal to noise ratio (SNR) and provides better performance in terms of receiver sensitivity [1]. Thus in this paper, 4-QAM mapping is selected for both downstream and upstream links in TWDM-PON [4].
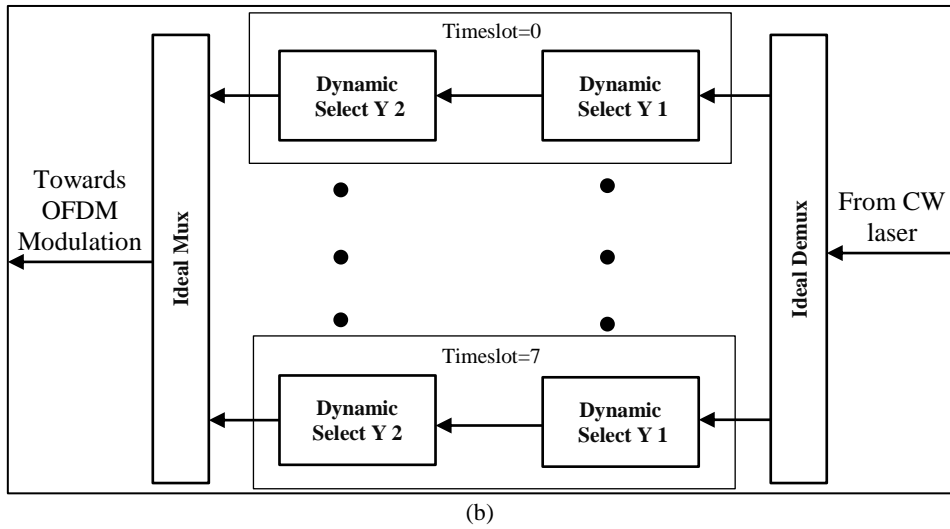
(a)

(b)

Fig. 2. Schematic of (a) the full-duplex 4×10Gbps TWDM- PON using 4-QAM-OFDM modulation and
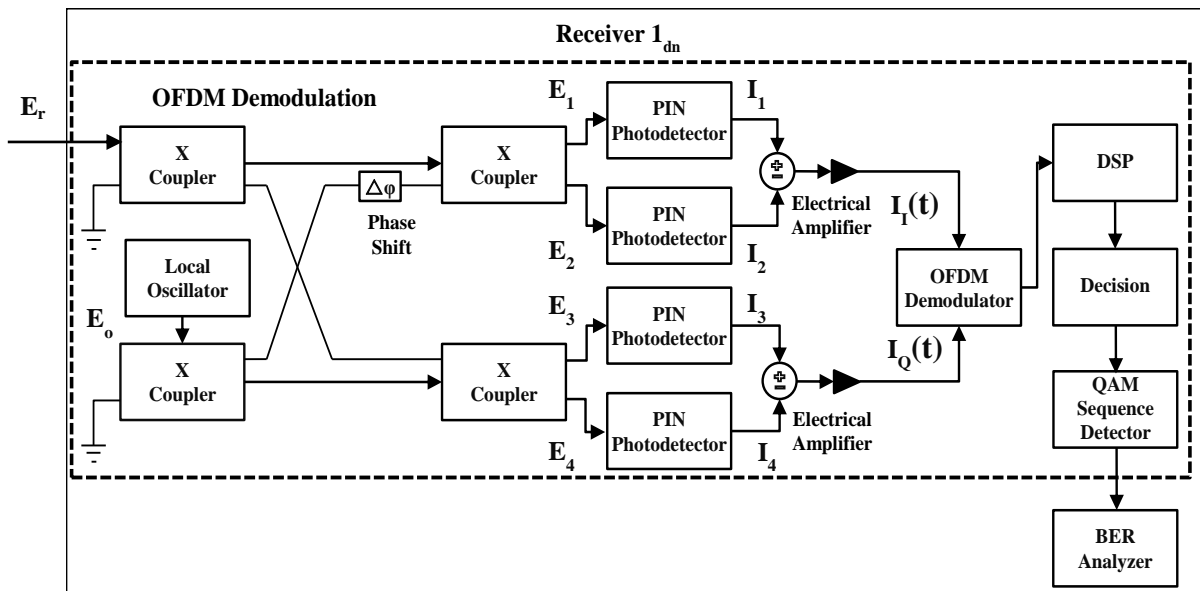*(b) upstream time switch section*

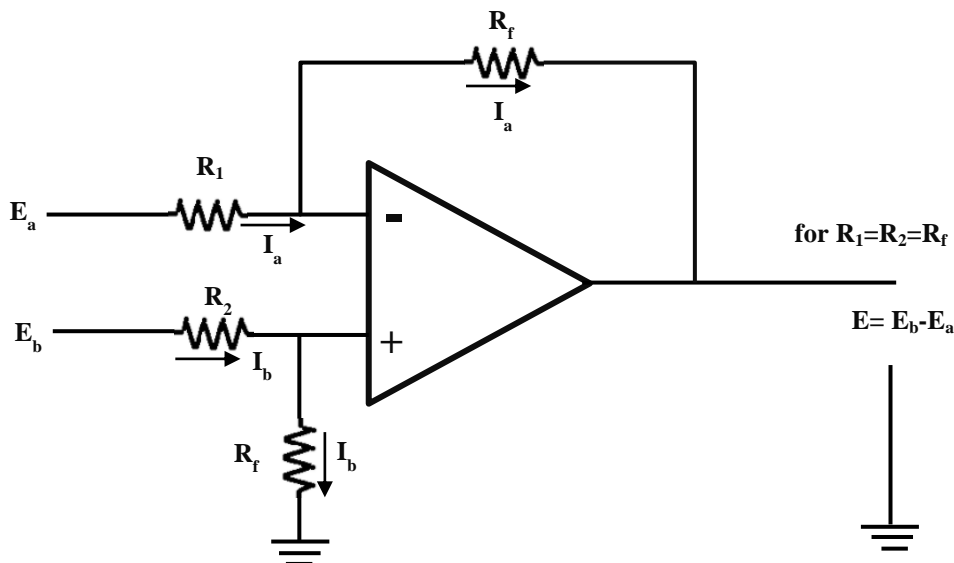*Fig. 3. Realization of an electrical substractor at receiver side*

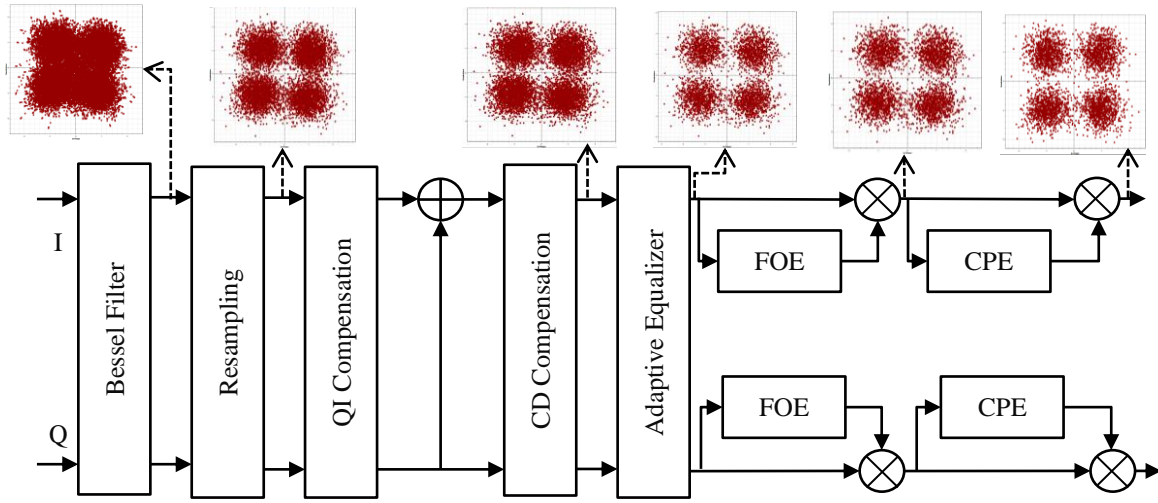*Fig. 4. Schematic of sub-components of electrical substractor*

Fig. 5. Single Polarization DSP unit along with constellation diagrams (color online)

The schematic for full-duplex 4×10Gbps TWDM PON system with 4-QAM-OFDM modulation over two 10-200 km fiber links is illustrated in Fig. 2. This system is realized using OptiSystem 16.0. In this work, the global parameters used for system design are number of samples and symbol rate i.e. 32768 and $2.5×10^9$ symbols per sec respectively. The CO has four pairs of transmitters and receivers. Both the downstream frequencies (187.8-187.5 THz) and the upstream frequencies (195.6-195.3 THz) are spaced by 100 GHz. These frequencies are emitted by utilizing four pairs of continuous wave (CW) lasers with a linewidth and phase noise of 0.15 MHz and -100 dBc/Hz respectively. One downstream transmitter presented in Fig. 2(a) comprises a pseudo-random bit sequence (PRBS) generator providing random binary sequences at 2.5-10 Gbps which are fed to 4-QAM with 2-bits per symbol sequence generator. The 4-QAM signal output is transmitted to an OFDM modulator for mapping over 512 subcarriers, through the serial to parallel converted. 512 subcarriers are employed with fast Fourier transform (FFT) having 1024 points and a cyclic prefix size of 64 [16]. Then OFDM modulator generates the in-phase (I) and quadrature (Q) components of the signal for further transmission in direct I/Q optical modulator. These I/Q components are filtered by a pair of low pass cosine roll-off filters having a roll-off factor of 0.2 then send for modulation. Here, the I/Q optical modulator comprises a CW laser, two pairs of electrical gain, a pair of mach-zehnder modulators (MZMs), and an optical power combiner [1]. Like this, four downstream TWDM-OFDM signals are multiplexed at different frequencies and transmitted over a fiber transmission link where it is constrained because of fiber attenuation, dispersion, and non-linearities effects. After this, the signal is directed to a bidirectional splitter, an optical amplifier, and directed to the receiver section where an opposite operation is carried out to demodulate the TWDM-OFDM signal. At the ONU side, a single user de-multiplexed signal is passed to the two pairs of X couplers (coupling coefficient=0.5) and

phase shift (phase shift=90^0) components for orthogonal coherent reception [17]. Then, the signal is fed to the two pairs of PIN photodetectors (PD), a pair of electrical substractor, a pair of an electrical amplifier (gain=20 dB) and OFDM demodulator, a digital signal processing (DSP) module for nonlinearities losses compensation, a decision component followed by a QAM sequence generator for coherent downstream traffic detection. The decision component proceeds the I and Q electrical signal channels received from the DSP, normalizes the electrical amplitudes of each I and Q channel to the respective 4-QAM grid and achieves a normalized threshold settings based decision on each received symbol. It performs the DC blocking, normalization, error vector magnitude (EVM) calculation, decision and calculates the symbol error rate respectively [18,19]. At the receiver, OFDM demodulator parameters should match with the transmitter to reconstruct the QAM symbols at the output side. The QAM sequence detector identifies the binary sequences and it is emulated with a communicated sequence to determine the Q-factor and bit error rate (BER) in a BER analyzer [2,12].

Fig. 3 shows the schematic of the realization of electrical substractor at coherent receiver side. The 90^0 phase shift will be generated among I and Q components by 90^0 optical hybrids and 180^0 phase shift between balanced detection. The optical hybrid output by ignoring loss and imbalance can be given as [3]

$$E_1 = \frac{1}{\sqrt{2}}[E_r + E_o] \tag{1}$$

$$E_2 = \frac{1}{\sqrt{2}}[E_r - E_o] \tag{2}$$

$$E_3 = \frac{1}{\sqrt{2}}[E_r - jE_o] \tag{3}$$

$$E_4 = \frac{1}{\sqrt{2}}[E_r + jE_o] \tag{4}$$

where E_r and E_o are the received optical signal and local oscillator input at coherent receiver. The photocurrents I_1 and I_2 from two photodetectors are as follows [3]

$$I_1 = \frac{1}{2}\{|E_r|^2 + |E_o|^2 + 2Re[E_r E_o^*]\} \quad (5)$$

$$I_2 = \frac{1}{2}\{|E_r|^2 + |E_o|^2 - 2Re[E_r E_o^*]\} \quad (6)$$

The final complex detected signal consisting in-phase along with quadrature phase components are expressed as

$$I(t) = I_I(t) + jI_Q(t) = 2E_r E_o^* \quad (7)$$

Fig. 4 shows the schematc of sub-components of electrical substractor at coherent receiver side. It consists of resistors and an operational amplifier. E_a and E_b are the input signals applied. I_a and I_b are the current flowing through R_1 and R_2 resistors respectively. Also feedback resistor, R_f is used to control the amount of output. Furher, Fig. 5 presents the diagram of single polarization DSP unit. Here, bessel filter is utilized with samples per symbol and bandwidth of 8×samples/bit and 0.75×symbol rate respectively. Resampling is attained at a rate of 4×samples/symbol. Quadrature (Q)-imbalance (I) compensation is used to reduce the phase and amplitude imbalances within I and Q signals respectively. Also, CD compensation is used to eliminate CD and fiber nonlinearity through the Back-Propagation algorithm. To perform a butterfly structure for de-multiplexing received signal polarization, adaptive equalizer is utilized. Frequency offset estimation (FOE) is used to eliminate the phase & frequency mismatch between the transmitter and the local oscillator. Whereas carrier phase estimation (CPE) is utilized to provide better output in terms of transmission range and bit rate. The signal received at the input of the DSP unit is given as [17]

$$X(k) = D(k). e^{j(2\pi \triangle fkT + \varphi_k)} + N(k) \quad (8)$$

where $D(k)$ and $N(k)$ mean the data symbol and zero-mean Gaussian random variable respectively. $\triangle f$, T and φ_k means carrier frequency offset, symbol period and carrier phase respectively. The received signal in terms of the fourth power can be represented as [17]

$$X^4(k) = B. e^{4j(2\pi \triangle fkT + \varphi_k)} + V(k) \quad (9)$$

where B and $V(k)$ denote constant amplitude and noise process with zero-mean respectively. Frequency offset can be evaluated by considering the signal's spectral density and it is given as [17]

$$X^4(k) = \frac{1}{4} arg\{\max[|S(f)|]\} \quad (10)$$

where

$$|S(f)| = \frac{1}{n}\sum_{k=0}^{n-1} B^4(k). e^{-j(2\pi \triangle fkT)} \quad (11)$$

where n denotes the block length. A decision component estimates the desired space $|d_{k,b}|^2$ to the nearest constellation point in the 2D complex plane as follows [17]

$$|d_{k,b}|^2 = |S_k e^{-j\varphi_b} - Y_{k,b}|^2 \quad (12)$$

where $Y_{k,b}$ means the decision $S_k e^{-j\varphi_b}$. At last, the received sequences are decoded for the polarization and then parallel to serial converted to obtain the output bits. Also the constellation diagrams show the benefit of using DSP unit in the proposed system. Again in the upstream transmission, 40Gbps OFDM signals are generated with four upstream frequencies. Here, the upstream 40Gbps traffic transmitted from the ONUs (at user end) and detected at the OLT side. The four independent upstream frequencies are transmitted by using four CW lasers with different switching times as shown in Fig. 2(b). In the upstream time switch section, each upstream wavelength uses an ideal demux, two cascaded dynamic selects Y (eight pairs) to transmit the information at defined timeslot and switching time an ideal mux. The switching time Ts_1 and Ts_2 are given respectively as [3]:

$$Ts_1 = Timeslot.\left(\frac{1}{Bit\ rate}\right).\left(\frac{Sequence\ length}{N}\right) \quad (13)$$

and

$$Ts_2 = Ts_1 + \left(\frac{Time\ window}{N}\right) \quad (14)$$

where N denotes the number of consumers. Here, N (=8), Timeslot (=0 to 7), Sequence length (=8192 bits), and Time window (=0.8192×10⁻⁰⁶s) are taken at a reference frequency of 193.4THz. The switching time of the proposed system is shown in Table 1.

Table 1. Switching Time of proposed the TWDM PON system using OFDM modulation for upstream transmission at 10Gbps

Timeslot	T_{s1} (s)	T_{s2} (s)
0	0	0.1024×10^{-06}
1	0.1024×10^{-06}	0.2048×10^{-06}
2	0.2048×10^{-06}	0.3072×10^{-06}
3	0.3072×10^{-06}	0.4096×10^{-06}
4	0.4096×10^{-06}	0.512×10^{-06}
5	0.512×10^{-06}	0.6144×10^{-06}
6	0.6144×10^{-06}	0.7168×10^{-06}
7	0.7168×10^{-06}	0.8192×10^{-06}

After passing the signals from the OFDM modulator and optical amplifier, each upstream wavelength is detected at the CO side using the OFDM demodulator. Also, to choose the latest simulation iteration a buffer selector is used along with DSP unit decision and BER analyzer. In this work, two separate SMF fiber links via bidirectional power splitter are utilized for isolating the upstream and downstream frequencies in the remote nodes

(RNs) as it reduces the Rayleigh backscattering (RB) noise interference in the proposed TWDM-PON system utilizing OFDM modulation [15]. Then, the downstream signals are de-multiplexed and distributed at a definite wavelength in the ONU section for detection, demodulation, and signal analysis. The various system parameters used in this proposed work are shown in Table 2.
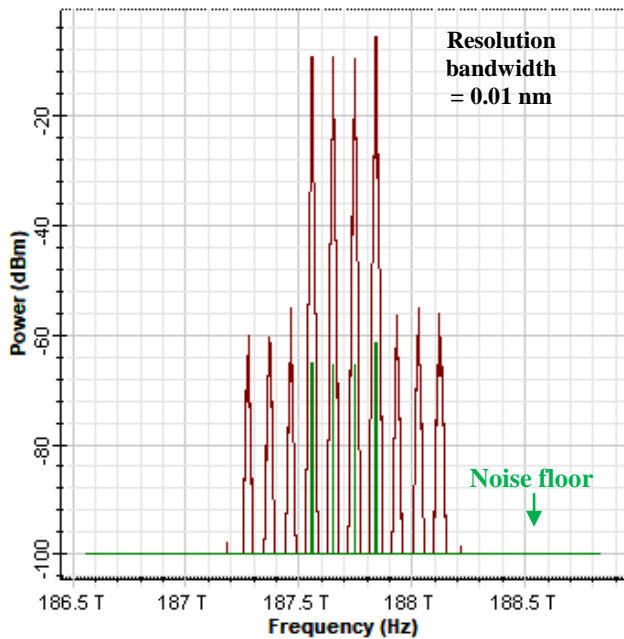
Table 2. Parameters of the proposed TWDM-PON employing 4-QAM OFDM modulation system

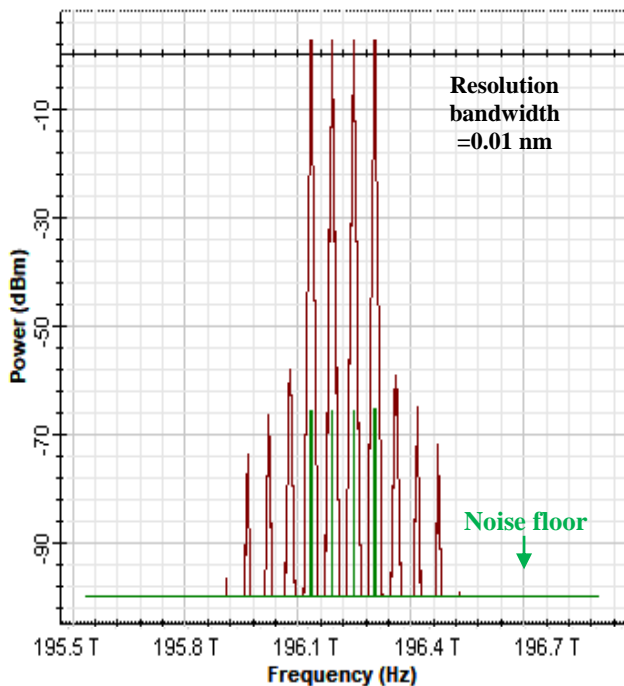| S.No.	Component Name	Component Parameters	Parameter Value	Unit
1	CW Laser	Input Power	-10 to 18	dBm
		Downstream frequency	187.8-187.5	THz
		Upstream frequency	195.6-195.3	THz
2	MZM Modulator	Extinction Ratio	60	dB
3	PRBS	Bit Rate	2.5-10	Gbps
4	OFDM modulator	Number of subcarriers	512	
		Number of FFT points	1024	
		Modulation index	4-QAM	
5	Optical amplifier	Gain	13	dB
		Noise figure	4	dB
6	PIN Photodetector	Responsivity	1	A/W
		Dark Current	10	nA
		Thermal Noise	1×10^{-22}	W/Hz
7	OFDM demodulator	Reference bit rate	2.5-10	Gbps
8	MUX/DEMUX	Insertion loss	0.3	dB
		Bandwidth	15	GHz
9	SMF	Reference frequency	193.4	THz
		Length	10-200	km
		Attenuation	0.2	dB/km
		Dispersion	16.75	ps/nm/km
		Dispersion slope	0.075	$ps/nm^2/k$
		Effective area	80	μm^2
		Nonlinear index of refraction	26×10^{-21}	m^2/W
		Temperature	300	K

3. Results and discussion

The performance of full-duplex TWDM-PON with 4-QAM OFDM modulation is investigated on the basics of Q-factor, BER, received optical power and EVM in percentage. The performance of the purposed system is analyzed for downstream OFDM (187.7THz) signal and upstream OFDM (195.5THz) signal at the receiver side over 10-200 km fiber link range, -10 to 18 dBm input power and 2.5-10 Gbps data rate. Fig. 6(a) and 6(b) present the optical spectra for OFDM signals in downstream and upstream directions respectively, which are obtained from an optical spectrum analyzer at -6 dBm input power for 40 Gbps TWDM-PON system. The noise floor is shown in green color with the resolution bandwidth of 0.01 nm.

(a)

(b)

Fig. 6. The optical spectra of OFDM signals in
(a) downstream and (b) upstream direction (color online)

3.1. Downstream system performance

This sub-section depicts the proposed system performance analysis for downstream transmission in the presence of fiber distortions and noise. Fig. 7 presents the Q-factor performance of downstream OFDM (187.7THz) signal in terms of increasing fiber link range (10-150 km)

at different data rates 2.5-10 Gbps with -6 dBm input power for the system.

The recent DSP algorithm based digital coherent receivers are implemented with most likely coded sequence. To achieve high data rate and long-reach distance, forward error correction (FEC) codes allow recovering the significant levels of error bits to provide an error free digital signal. The FEC enhancement uses soft or hard decision algorithms that provide optimum net coding gain (NCG), improved tolerance to channel impairments or noise, high transmission capacity upto 100 Gbps with 7%-35% overhead. Thus, in this paper, hard decision FEC with 7% overhead is utilized that provides 6 dB gain and hence increment in the minimum BER value i.e. from 10^{-9} to 3.8×10^{-3} under 7% FEC [20–23]. The dotted line at Q-factor of presents the lowest Q-factor value for the successful reception of the signal to accomplish the minimum 3.8×10^{-3} BER under 7% FEC [24]. An improvement in Q-factor gives deterioration in BER value and better network performance.

From the results reported in Fig. 7, it can be seen that as the fiber length increases, the performance of the received signal deteriorates in terms of transmission Q-factor for all channels at 2.5 Gbps, 5 Gbps, and 10 Gbps data rates. The proposed system performs best at 2.5 Gbps data rate. It is reported that the Q-factor at 2.5 Gbps is measured as 51.47, 51.27, and 1.11 whereas at 5Gbps is measured as 50.95, 50.72, and 0.74 and at 10 Gbps is measured as 51, 4.67 and 0.48 at a fiber link range of 10 km, 90 km, and 150 km respectively. The results observed demonstrate a faithful transmission of the system at 2.5 Gbps, 5 Gbps, and 10 Gbps transmission rates over fiber link range of 120 km, 110 km, and 90 km respectively under the minimum BER of 3.8×10^{-3}. Further, the sharp decays in the Q-factor over 110 km, 100 km and 50 km at 2.5 Gbps, 5G bps and 10 Gbps respectively are due to the fiber impairments.

The various impairments mainly accountable for the decline in the Q-factor values are attenuation, CD, fiber nonlinearities and noise, causing in the decrease of the signal quality [25]. Fig. 7 also presents the constellation diagrams of the proposed TWDM-PON system with 4-QAM OFDM modulation over the 10-150 km fiber link at 2.5 Gbps. It can be seen that signal distortion deteriorates at a lower transmission rate and the signal can be successfully regenerated at the receiver.
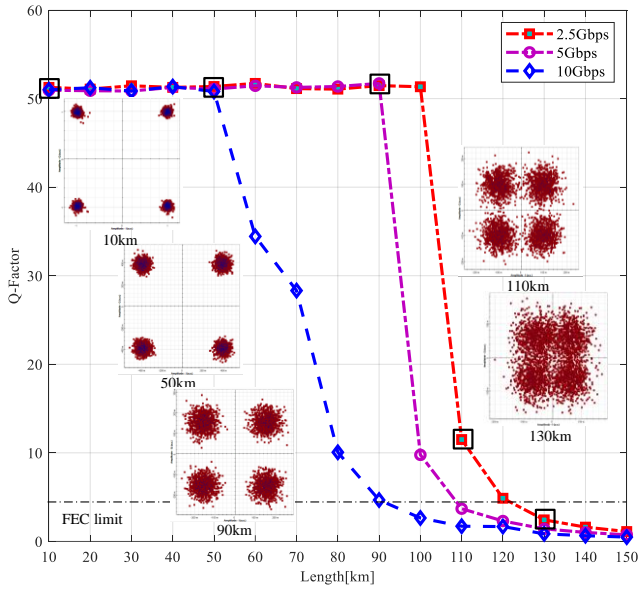
Fig. 7. Q-Factor versus fiber length at different data rate with constellation diagrams of 2.5 Gbps downstream signal for different fiber lengths (color online)
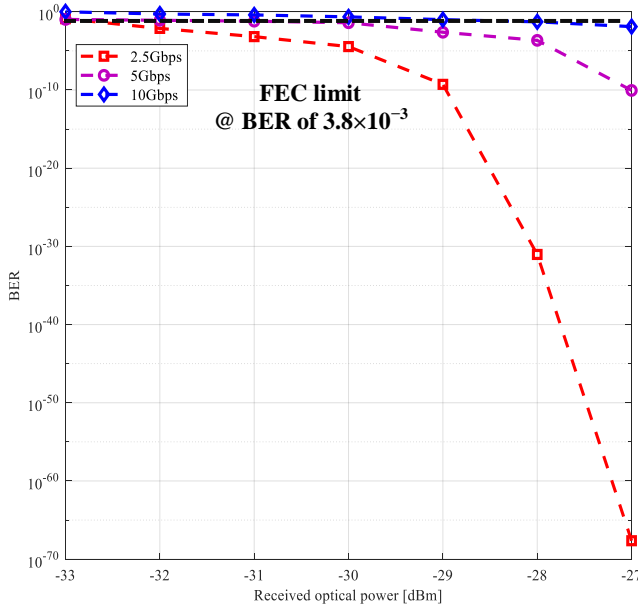

Fig. 8. BER versus received optical power for downstream signals at the various data rate (color online)

Fig. 8 presents the BER versus received optical power (-27 to -33 dBm) over 10 km fiber link range of downstream signal for the symmetric TWDM-PON with OFDM modulation system at 2.5 Gbps, 5 Gbps and 10Gbps information rate. From the results reported in Fig. 8, it can be seen that as the received optical power increases, the performance of the received signal improves in terms of minimum BER value for the downstream channel at various data rates. It is noticed that the BER value of downstream OFDM signal at 2.5 Gbps is computed as $2.27×10^{-68}$, $3.57×10^{-5}$ and $1.32×10^{-1}$; at 5 Gbps it is computed as $8.82×10^{-11}$, $3.98×10^{-2}$ and

$1.06×10^{-1}$ whereas at 10 Gbps it is computed as $1.27×10^{-2}$, $3.24×10^{-1}$ and 1 at the received optical power of -27dBm, -30dBm and -33 dBm respectively. It is also reported that the proposed system performs best at 2.5 Gbps data rate due to minimum signal distortion at a lower transmission rate. The observed results demonstrate a faithful data transmission with acceptable BER value ($3.8×10^{-3}$ under 7% FEC) for the received optical power of -27 to -32 dBm, -27 to -29 dBm and -27 dBm at 2.5 Gbps, 5 Gbps, and 10 Gbps data rates respectively.
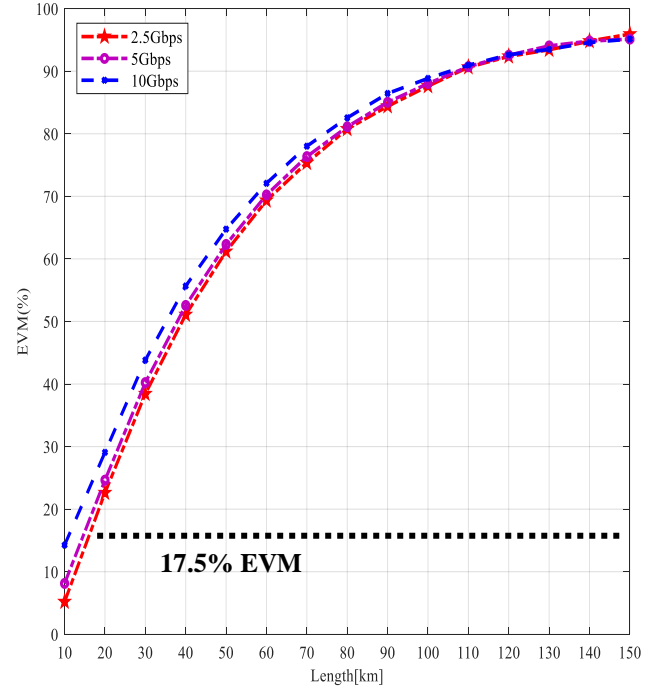

Fig. 9. EVM (%) versus length of downstream OFDM signal for 40 Gbps TWDM-PON system using OFDM modulation (color online)
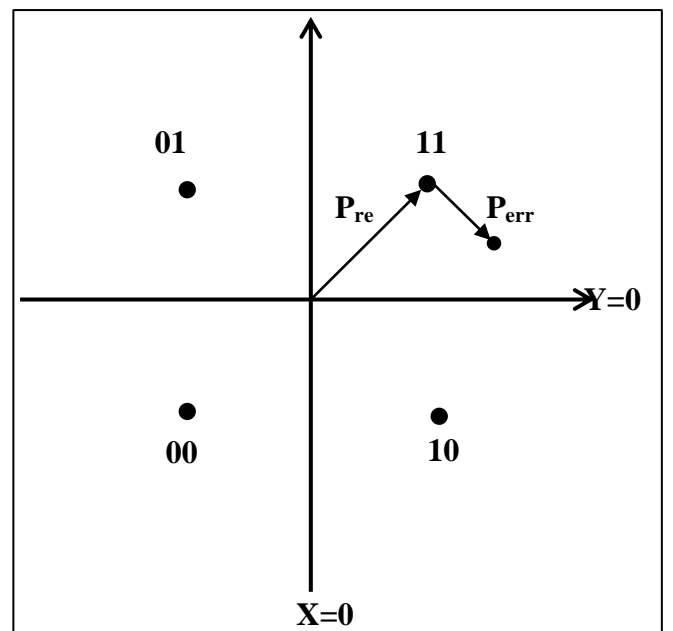

Fig. 10. Error vector magnitude computation

Fig. 9 presents the EVM (%) versus fiber length at -6dBm input power at 2.5-10Gbps data rates. EVM is utilized to compute the received signal quality under the effect of fiber distortion and is determined from the constellation diagram. EVM is generally illustrated in percentage (%) and the EVM(%) of the received signals is measured as follows [26]

$$EVM(\%) = \sqrt{\frac{\overline{\left|S-\lfloor S \rfloor_d \right|^2}}{\left|s_d\right|^2}} \times 100\% \qquad (15)$$

where S and $\lfloor S \rfloor_d$ mean the symbol sequence and decision of S respectively, and $\overline{(\dots)}$ presents the mean value. Also, the threshold boundaries (x=0; y=0) based decision algorithm for 4-QAM modulation format achieves a hard decision on the received symbols as shown in Fig. 10.

From the results reported in Fig. 9, it can be noticed that the EVM values increase as the transmission distance increases. For 4-QAM format, the dotted line shows the EVM limit defined in 3rd generation partnership project (3GPP) specifications [27]. EVM(%) for 2.5 Gbps is measured as 5.20, 84.40, and 95.02 whereas for 5 Gbps is measured as 8.13, 85.03, and 95.13 and for 10 Gbps is measured as 14.26, 86.44 and 95.94 at a fiber link range of 10 km, 90 km, and 150 km respectively. At 150 km transmission distance, the Q-factor corresponding to EVM(%) values 95.02, 95.13, and 95.94 are 1.11, 0.72, and 0.48 respectively causing in the decrement in Q-factor. Although, at 10km transmission distance almost 2% and 10% enhancement in EVM is measured as data rate increments from 2.5 Gbps to 5G bps and 2.5 Gbps to 10Gbps respectively. This degrades Q-factor from 51.72 to 51.47 and 51.72 to 51 for increment of bit rate from 2.5 Gbps to 5 Gbps and 2.5 Gbps to 10 Gbps respectively. Thus, it is observed that for a lower data rate, EVM(%) reduces due to the improvement in the received power resulting in enhanced system performance. EVM is influenced by a broad range of issues like in-phase/quadrature-phase mismatches in the modulator/demodulator components because of dc offset, gain as well as phase differences. Moreover, phase noise and frequency offset also lead to a constellation diagram with misplaced points causing worse modulation quality and more errors [26].
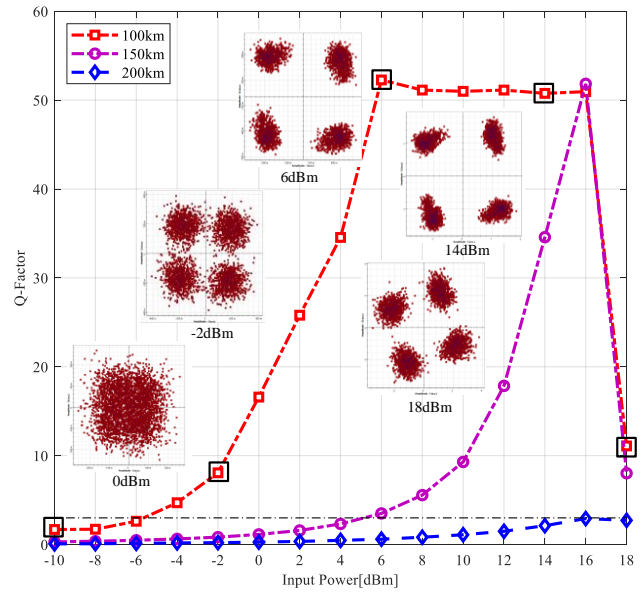

Fig. 11. Q-Factor versus input power at various fiber lengths (100-200 km) of downstream signal with constellation diagrams over 100 km fiber link at different input powers (color online)

Fig. 11 presents the Q-factor versus input power (-10 to 18 dBm) over 100-200 km fiber link range of downstream signal for symmetric 40 Gbps TWDM-PON with OFDM modulation system. It is seen that Q-factor value improves with the rise in optical input power up to 6 dBm, 16 dBm and 16 dBm over 100 km, 150 km, and 200 km fiber link respectively beyond which it again decreases. The decrease in Q-factor after 6 dBm and 16 dBm is because of the dominant nonlinear effects in the fiber at high input power. The figure reported that in the proposed system, Q-factor is measured as 1.69, 52.27, and 11.09 over 100 km whereas it is measured as 0.30, 3.50, and 8.02 over 150 km and it is measured as 0.07, 0.60 and 2.72 over 200 km at an input power of -10 dBm, 6 dBm and 18 dBm respectively. It is observed that in TWDM-PON using OFDM modulation, Q-factor for 100 km fiber link range maximum increases to 52.27 (at 6 dBm) with the increase in launch power and decreases with further increase in input power. Whereas, for 150 km and 200 km fiber link ranges, the maximum achieved Q-factor values are 51.83 and 2.92 respectively. Thus, the obtained results demonstrate the best performance of the proposed TWDM-PON system at 6dBm input power over 100 km fiber link range followed by transmission distance of 150 km and 200 km. Fig. 11 also illustrates the constellation diagrams of the proposed system at a 10 Gbps data rate over 100 km fiber link at different input powers. It is interpreted that the distortion of the signal decreases up to optimum input power and then again increases with an increase in input power. Also, the received signal can be successfully regenerated at the receiver side from -6 dBm to 18 dBm, 6 dBm to 18 dBm, and at 16 dBm over 100 km, 150 km and 200 km respectively. The comparative performance of the downstream signal at 10 Gbps for

varying input power over the 100-200 km fiber range is summarized in Table 3.

Table 3. Comparative performance of downstream link for varying input power and fiber length

Length (km)	Input power (dBm)	BER	Received optical power (dBm)
100	-10	1.21×10^{-1}	-30.44
	-6	4.33×10^{-3}	-26.59
	-2	3.28×10^{-16}	-22.65
	2	3.67×10^{-147}	-18.68
	6	0	-14.69
	10	0	-10.69
	14	0	-6.69
	18	6.71×10^{-29}	-2.71
150	-10	3.81×10^{-1}	-39
	-6	3.13×10^{-1}	-35.91
	-2	2.02×10^{-1}	-32.37
	2	5.64×10^{-2}	-28.55
	6	2.26×10^{-4}	-24.64
	10	7.16×10^{-21}	-20.67
	14	2.07×10^{-262}	-16.69
	18	5.16×10^{-16}	-12.71
200	-10	4.71×10^{-1}	-43.07
	-6	4.46×10^{-1}	-42.07
	-2	4.12×10^{-1}	-40.25
	2	3.61×10^{-1}	-37.56
	6	2.71×10^{-1}	-34.19
	10	1.35×10^{-1}	-30.50
	14	1.67×10^{-2}	-26.62
	18	3.24×10^{-3}	-22.68

The above-reported results show that optimum input power is desirable for increasing the downstream fiber link in the proposed system.

3.2. Upstream system performance

This sub-section depicts the performance analysis of the proposed system for upstream link under the influence of different fiber impairments and noise.
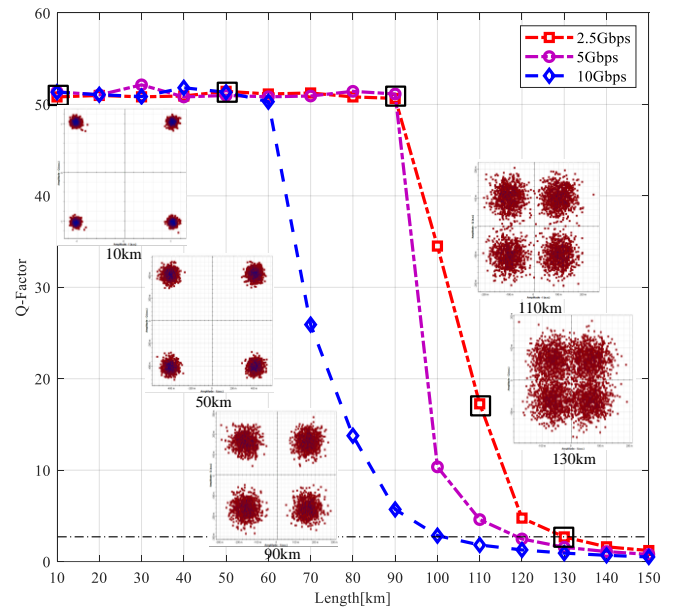

Fig. 12. Q-Factor versus fiber length at various data rate with constellation diagrams for upstream 2.5 Gbps bit rate at different fiber lengths (color online)

Fig. 12 reports the Q-factor of the received upstream OFDM (195.5 THz) signal as a function of increasing fiber link range (10-150 km) at different data rates 2.5-10 Gbps with -6 dBm input power for the proposed system. The results mentioned show that the maximum fiber link range of the proposed system with acceptable Q-factor for the upstream signal at 2.5 Gbps, 5 Gbps and 10 Gbps is 130 km, 120 km and 100 km respectively. Also, the abrupt decay in the Q-factor at 100 km is seen for both 2.5 Gbps and 5 Gbps data rates while at 60 km the decay is observed for 10 Gbps data rate because of the fiber nonlinearities. Fig. 12 also presents the constellation diagrams of the proposed TWDM-PON system with OFDM modulation at 2.5 Gbps data rate over 10-150 km fiber link range. These diagrams interpreted that the received signal distortion increases with an increase in fiber link and the proposed system performs best at 2.5 Gbps transmission rate.
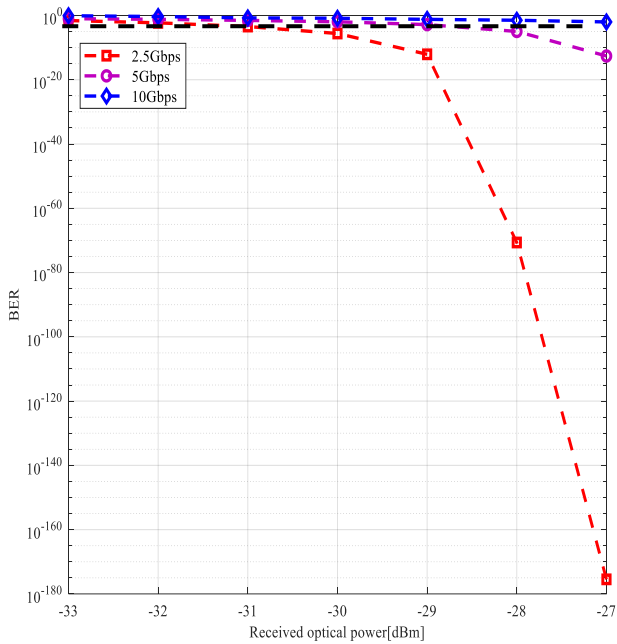
Fig. 13. BER versus received optical power for the upstream link at the various bit rate (color online)

Fig. 14. EVM (%) versus length of upstream OFDM signal for 40Gbps TWDM-PON system (color online)

From the Fig. 13, it is noticed that the best BER value for upstream 2.5 Gbps data rate is computed as 34.05×10^{-177}, 2.49×10^{-6} and 2.68×10^{-2} whereas the worst BER value for upstream 10 Gbps data rate is reported as 9.83×10^{-3}, 1.36×10^{-1} and 8.37×10^{-1} at the received optical power of -27 dBm, -30 dBm and -33 dBm respectively corresponding to the fiber link range of 10 km. It is reported that the proposed system performs best at 2.5 Gbps data rate and worst at 10 Gbps data rate. The results presented demonstrate a reliable data transmission with acceptable BER value for the received optical power of -27 to -32 dBm, -27 to -29 dBm and -27 dBm at 2.5 Gbps, 5 Gbps, and 10 Gbps data rates respectively.

The results reported in Fig. 14 demonstrate a faithful fiber link range for 2.5 Gbps, 5 Gbps and 10 Gbps data rates over a fiber link range of 10-150 km in terms of EVM(%) for the 40 Gbps TWDM-PON system. At 10 km transmission distance, EVM(%) measured is 5.89, 7.05 and 11.43 for 2.5 Gbps, 5 Gbps and 10 Gbps data rate respectively. The Q-factor corresponding to EVM(%) values 5.89, 7.05 and 11.43 are 51.38, 51.34 and 50.82 respectively causing in the decrement in Q-factor. With an increase in fiber length, Q-factor further decreases due to almost 1% and 5% improvement in EVM as data rate increases from 2.5 Gbps to 5 Gbps and 2.5 Gbps to 10 Gbps respectively. Thus, it is observed that for 2.5 Gbps data rate, EVM(%) value is minimum followed by 5 Gbps and 10 Gbps data rate respectively.
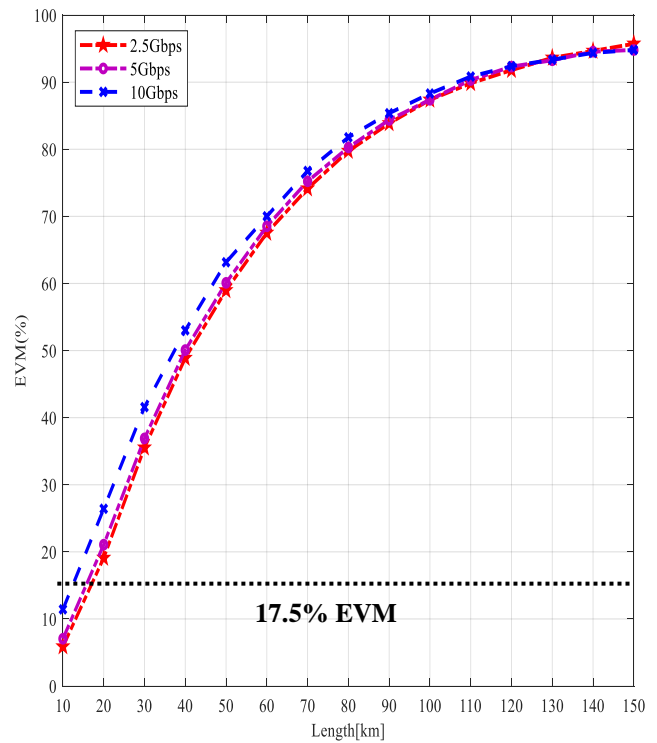

Fig. 15. Q-Factor versus input power at various fiber lengths (100-200 km) for the upstream *signal with constellation diagrams over 100 km fiber link at different input powers (color online)*

Fig. 15 represents the Q-factor versus input power (-10 to 18 dBm) over 100-200 km fiber link range for upstream signals in 40Gbps proposed TWDM-PON system. The observed results demonstrate an optimum performance of the proposed system for the upstream signal at 6 dBm, 14 dBm and 16 dBm input power over 100 km, 150 km and 200 km respectively. Fig. 15 also presents the constellation diagrams of the symmetric 40G bps TWDM-PON with OFDM modulation system over

100 km fiber link at different input power from -10 to 18 dBm. From these diagrams, it is interpreted that the upstream signal can be recovered at the receiver at different input powers. The comparative performance of the upstream link for varying input power over the 100-200 km fiber range is summarized in Table 4.

Table 4. Comparative performance of upstream link for varying input power and fiber length at 10 Gbps data rate

Length (km)	Input power(dBm)	BER	Received optical power(dBm)
100	-10	1.00×10^{-1}	-30.03
	-6	1.46×10^{-3}	-26.16
	-2	6.30×10^{-23}	-22.30
	2	2.11×10^{-259}	-18.25
	6	0	-14.26
	10	0	-10.26
	14	0	-6.27
	18	0	-2.29
150	-10	3.75×10^{-1}	-38.60
	-6	2.97×10^{-1}	-35.52
	-2	1.89×10^{-1}	-31.96
	2	4.08×10^{-2}	-28.14
	6	1.06×10^{-5}	-24.21
	10	1.06×10^{-38}	-20.25
	14	0	-16.26
	18	2.90×10^{-6}	-12.69
200	-10	4.70×10^{-1}	-42.87
	-6	4.44×10^{-1}	-41.80
	-2	4.06×10^{-1}	-39.96
	2	3.49×10^{-1}	-37.18
	6	2.47×10^{-1}	-33.81
	10	1.16×10^{-1}	-30.06
	14	9.73×10^{-3}	-26.19
	18	1.25×10^{-2}	-22.20

The above-demonstrated results show that optimum input power is desirable for increasing the upstream fiber link in the proposed system under the influence of fiber distortions. This work shows the significant enhancement as compared to present work in [28] where the maximum achievable fiber link range at 10 Gbps data rate at -4 dBm input power is 60 km and [29] where the maximum acceptable fiber link range is 20 km at 10 Gbps transmission rate at an input power of -5 dBm. Also, [13] presents the work at the 10 Gbps data rate, where the successful total link distance is 20 km at -6 dBm input power. Besides this, Table 5 shows the proposed scheme comparison to already existing techniques and it presents that proposed system shows the supreme performance in terms of system complexity, transmission distance, data rate and system deployment cost. The performance comparison of downstream and upstream links for maximum faithful fiber link and optimum input power in the presence of fiber distortions is compiled in Table 6 and Table 7 respectively.

To summarize the above-analyzed results reported that in the NG-PON2 based proposed TWDM-PON with 4-QAM OFDM modulation system, the information transmission in upstream link outperforms downstream link. This is because downstream link is more influenced by adjacent channel disturbances and fiber distortions than upstream link because downstream data is delivered on the basics of WDM multiplexing scheme which is more susceptible to channel impairments. Whereas the upstream transmission uses a single wavelength based on the TDM multiplexing scheme with different time slots which increase the channel capacity causes minimum distortion.

Table 5. Proposed scheme comparison to already existing techniques

Reference	Technique used	Complexity	Maximum Transmission distance (km)	Maximum data rate (Gbps)	Deployment cost
[30]	Selected mapping (SLM) in OFDM-PON	Low	100	8.9	Low
[31]	Feld programmable gate array (FPGA)-based OFDM	Moderate	30	50	Moderate
[32]	4-QAM-OFDM-PON	Low	190	10	Low
Proposed architecture	TWDM-PON employing 4-QAM-OFDM modulation	Low	200	40/40	Low

Table 5 shows that the earlier reported strategies use the OFDM-PON with different schemes such as SLM, FPGA etc. up the highest data rate of 50 Gbps, 190 km transmission distance with low or moderate development complexity as well as deployment cost. While in the proposed TWDM-PON architecture employing 4-QAM-OFDM modulation offers the high data rate of 40 Gbps over 200 km maximum transmission distance with low complexity and low deployment/installation cost. Hence the proposed system provides significant benefits such as high bandwidth, cost-effectiveness, easy installation, scalability as well as easy upgradeability.

Table 6. Performance comparison of downstream and upstream links for maximum achievable fiber link for -6dBm input power

Bit rate (Gbps)	Maximum transmission range (km) @ BER of 10^{-3}	
	Downstream	Upstream
2.5	120	130
5	110	120
10	90	100

Table 7. Performance comparison of downstream and upstream links for optimum input power over fiber link at 10Gbps data rate

Length (km)	Optimum input power (dBm) with acceptable BER	
	Downstream	Upstream
100	6	6
150	16	14
200	16	16

4. Conclusion

In this paper, a next-generation full-duplex 4×10 Gbps TWDM-PON with 4-QAM OFDM modulation system over 10-200 km has been proposed and analysed for high data rate and long-reach and applications. In the proposed system, DSP unit has been realized to compensate the channel impairments. Using this, downstream and upstream 4-QAM OFDM modulated signals at 2.5 Gbps have been transmitted over 120 km and 130 km fiber length respectively with acceptable BER of 3.8×10^{-3} under 7% FEC. The bidirectional transmission distance and data rate can be further increased up to 200 km and 40/40 Gbps bit rate respectively at 16 dBm system input power. For both downstream and upstream link the maximum received optical power is -27 dBm at 10 Gbps data rate over 10 km fiber link. Moreover, upstream link shows better performance than downstream link in terms of EVM

values for variable data rate from 2.5 Gbps to 10 Gbps. The comparative performance of the proposed system also shows its superiority as compared to previous work. Thence, the TWDM-PON with OFDM modulation can enhance the fiber link utilization and achieve a smooth upgradation to NG-PON3 requiring more than 40/40 Gbps data rate from rural areas to urban areas.

References

[1] V. Kachhatiya, S. Prince, Opt. Fiber Technol. **32**, 71 (2016).
[2] V. Kachhatiya, S. Prince, Opt. Laser Technol. **104**, 90 (2018).
[3] M. Kumari, R. Sharma, A. Sheetal, J. Opt. Commun. **0**, 1 (2019).
[4] C. H. Yeh, C. W. Chow, H. Y. Chen, Y. L. Liu, Opt. Fiber Technol. **20**, 84 (2014).
[5] B. Lin, Y. Li, S. Zhang, X. Tang, Opt. Fiber Technol. **26**, 206 (2015).
[6] M. Šprem, D. Babić, Opt. Commun. **451**, 1 (2019).
[7] X. Tang, J. Zhou, M. Guo, J. Qi, F. Hu, Y. Qiao, Y. Lu, Opt. Fiber Technol. **40**, 108 (2018).
[8] W. F. Zhang, X. J. Xin, Q. Zhang, Z. X. Zhang, W. Nai, Y. Shi, J. China Univ. Posts Telecommun. **17**, 125 (2010).
[9] Y. Shao, F. Chen, A. Wang, Y. Luo, L. Chen, Optik **146**, 63 (2017).
[10] H. K. Gill, G. K. Walia, N. S. Grewal, Optik **177**, 93 (2019).
[11] S. Selvendran, A. Sivanantha Raja, K. Esakki Muthu, A. Lakshmi, Wirel. Pers. Commun. **109**, 1377 (2019).
[12] A. Kaur, B. Kaur, K. Singh, Optik **134**, 287 (2017).
[13] W. C. Lyu, A. Wang, D. Xie, L. Zhu, X. Guan, J. Wang, J. Xu, Opt. Commun. **414**, 77 (2018).
[14] A. Grover, A. Sheetal, Optoelectron. Adv. Mat. **14**, 136 (2020).
[15] B. Lin, Y. Li, S. Zhang, X. Tang, Opt. Fiber Technol. **26**, 206 (2015).
[16] N. Kalikulov, D. Zhussip, N. Zhexenov, R. C. Kizilirmak, Wirel. Pers. Commun. **112**, 2715 (2020).
[17] H. Yang, J. Li, B. Lin, Y. Wan, Y. Guo, L. Zhu, L. Li, Y. He, Z. Chen, J. Light. Technol. **31**, 3035 (2013).
[18] H. Yang, J. Ye, Y. Liu, L. Yan, Opt. Fiber Technol. **24**, 127 (2015).
[19] M. Singh, J. Malhotra, M. S. Mani Rajan, V. Dhasarathan, M. H. Aly, Alexandria Eng. J. **59**, 977 (2020).
[20] G. Tzimpragos, C. Kachris, I. B. Djordjevic, M. Cvijetic, D. Soudris, I. Tomkos, IEEE Commun. Surv. Tutorials **18**, 209 (2016).
[21] M. Reza Salehi, S. Farhad Taherian, J. Opt. Soc. Korea **18**, 65 (2014).
[22] L. Li, G. Xiao-Bo, L. Jing, J. Opt. Commun. **37**, 93 (2016).
[23] A. Alvarado, E. Agrell, D. Lavery, R. Maher, P. Bayvel, J. Light. Technol. **34**, 707 (2016).
[24] Y. Wei, J. He, R. Deng, J. Shi, S. Chen, L. Chen, Opt.

Commun. **405**, 329 (2017).

[25] K. Mallick, R. Mukherjee, B. Das, G. C. Mandal, A. S. Patra, AEU - Int. J. Electron. Commun. **96**, 260 (2018).

[26] A. Sheetal, H. Singh, Opt. Quantum Electron. **50**, 1 (2018).

[27] D.-N. Nguyen, J. Bohata, J. Spacil, D. Dousek, M. Komanec, S. Zvanovec, Z. Ghassemlooy, B. Ortega, Opt. Express **27**, 33745 (2019).

[28] S. Sharma, D. Parkash, S. Singh, ICRIC 2019, **597**, 365 (2020).

[29] C. H. Kim, S. M. Jung, S. Y. Jung, S. M. Kang, S. K. Han, Opt. Fiber Technol. **27**, 35 (2016).

[30] Y. Xiao, Z. Wang, J. Cao, R. Deng, Y. Liu, J. He, L. Chen, J. Opt. Commun. Netw. **10**, 46 (2018).

[31] X. Chen, M. Gao, Y. Sha, J. Zhang, E. Fang, H. Ren, IEEE Access **7**, 173731 (2019).

[32] G. Pandey, A. Goel, J. Opt. Commun. **38**, 461 (2017).

_____

[*]Corresponding author: meetkumari08@yahoo.in